NUMERICAL STUDIES OF SPRAY BREAKUP IN A GASOLINE DRIECT INJECTION (GDI) ENGINE

by

Samad JAFARMADAR, Vahied. **HEIDARPOOR**

The objective of this study is to investigate Spray Breakup process of sprays injected from single and two-hole nozzles for gasoline direct Injection (GDI) engines by using three dimensional CFD code. Spray characteristics were examined for spray tip penetration and other characteristics including: the vapor phase concentration distribution and droplet spatial distribution, which were acquired using the computational fluid dynamics (CFD) simulation. Results showed that as the hole-axis-angle (γ) of the two-hole nozzle decreased, the droplet coalescence increased and vapor mass decreased. The spray with cone angle (θ_0) 5 deg for single hole nozzle has the longest spray tip penetration and the spray with the γ of 30 deg and spray cone angle θ_0=30 deg for two hole nozzles had the shortest one. Also, when the spray cone angle (θ_0) and hole–axis-angle (γ) increased from 5 to 30 deg, the Sauter mean diameter (SMD) decreased for both single-hole and two-hole nozzles used in this study. For a single-hole nozzle, when spray cone angle increased from 5 to 30 deg, the vaporization rate very much because of low level of coalescence. The result of model for tip penetration is good agreement with the corresponding experimental data in the literatures.

Keywords: *DGI, Spray, Numerical simulation, Hole-type nozzle*

1. Introduction

In the last twenty years the fuel system of spark ignition (SI) engines has evolved monotonically from carburetion to throttle-body injection, then to simultaneous-fire port-fuel injection (PFI), and more recently to phased sequential-fire PFI. Advanced systems such as variable valve-timing, multiple roller camshaft, computer algorithms for transient metering, turbo-charging have also been incorporated. But the current high-technology PFI engine, although highly evolved, has nearly reached the limit of the potential since it still uses throttling for load control and it still has a film of liquid fuel in the intake ports. The gasoline direct injection (GDI), in theory, does not have these two limitations and offers many opportunities for achieving significant improvements in engine fuel consumption and emissions reductions [1,2].

Gasoline port-fuel injection engines that are in production today have a higher BSFC compared to the direct-injection (DI) Diesel engine. This is due to the higher compression ratio and the unthrottled operation typical of diesel engines, that, however, have higher NOx and soot emissions, slightly higher noise level and lower startability. The ideal would be to put together the best features of the both combining Diesel efficiency with gasoline specific power. Studies in this direction have shown that this may be achieved with gasoline direct injection (GDI) unthrottled engine. Fuel is

injected directly into the combustion chamber in order to have a mixture with an ignitable composition near the spark plug at the time of ignition for all loads.

In a GDI engine, the fuel is injected directly into the cylinder avoiding the problems related with fuel film in the port. However this does not guarantee that fuel film problems are absent: the wetting of the piston crown or other combustion chamber surfaces, whether intentional or not, may occur. The mass delivered into the cylinder is more accurately controlled, providing potential for leaner combustion and less cycle-to-cycle variations. GDI engines require much less fuel to start leading to reductions in hydrocarbons spikes during transient operations that could approach the level observed for steady operating conditions [3]. Other advantages of the GDI are the fuel cut-off in deceleration and the cooling of the inducted charge. The evaporation of the fuel droplets cools the air and this allows higher compression ratios and lowers the octane requirement of fuels, and, in addition, if the injection occurs during the induction event also the volumetric efficiency can be enhanced. Another limitation of PFI is the use of throttling for load control that in the GDI engine is obtained varying the amount of fuel injected.

In spite of the potential advantages mentioned above the development of GDI engines has encountered many obstacles that hinder its application. The injection of fuel in the cylinder reduces the time available for evaporation and mixing. The PFI engines have the advantage that the intake system acts as a prevaporizing chamber. In GDI engines the time is reduced so fuel spray atomization has to be an order of magnitude finer, so that higher injection pressures are necessary. Moreover, the high NOx ,HC and particulate emissions at high load, and the fact that a three way catalyst cannot be effectively used. Even if the engine operates at an overall lean condition that reduces NOx emission the level is still high compared to the level obtained with a three way catalyst, so much work has been made and is still needed to develop lean NOx catalyst. The most important obstacle in the development of GDI engines is that the control of the stratified-charge combustion over the entire operating range is very difficult. Since the location of the ignition source is fixed in SI engines and the mixture cloud must be controlled both temporally and spatially for a wide range of operating conditions. The development of a successful combustion system depends on the design of the fuel injection system and the matching with the in-cylinder flow field.

As a potential alternative to conventional port fuel injection (PFI) gasoline engines, direct-injection spark-ignition (DISI) engines are getting more and more interests for their significantly enhanced fuel economy, transient response, and cold-start hydrocarbon emission levels [1]. For a DISI engine, one of the most crucial processes is the spray and mixture formation process because whether the injected fuel can be atomized in a very short time and can provide a combustible mixture at the spot of spark plug at discharging time will greatly affect the whole combustion process and engine performance. The DISI systems fall into three categories according to the dominant approach of the stratified charge process: spray-guided, wall-guided, and flow-guided [4]. The wall-guided system has been implemented in the commercial DISI engines [5, 6]. In this system, due to the non-vaporized fuel conflicting the piston cavity wall, a fuel film is formed on the wall inevitably, thus resulting in an increase in both soot and unburned hydrocarbon emissions [7, 8]. In a flow-guided system, in order to ensure that the ignition occurs at a thermodynamic optimum timing, a stable airflow is required to enhance the mixture formation inside the spray cloud and to transport the compact spray cloud to the sparkplug. However, within the stratified operation range, it is impossible to generate such a stable airflow under all engine operating conditions. In addition, the generation of a swirl or tumble increases

losses due to throttling and thus reduces fuel economy. For both the wall-guided system and the flow-guided system, the complex shape of the piston crown increases the surface area and results in an increase in the heat loss. Furthermore, the sharp edges of the piston make the knock resistance deteriorated [9] and the compression ratio often has to be lowered than that of a flat piston in order to prevent knock at full load. However, the spray-guided system which is called the next-generation DISI system by some researchers, showed its potential of solving the problems above in the wall-guided system and the flow-guided system [10]. Compared with the outwardly opening nozzle and pressure-swirl injector, the spray structure of the multi-hole nozzle does not change with increasing backpressure [11], which is an important criterion for the realization of the spray-guided DISI engine. Although the multi-hole nozzles have met with success in DI diesel engines, at the early stage of the development of DISI engines, they resulted in the poor engine performance. Their excessive long penetrations and large droplet sizes led to a great deal of soot, CO and HC emissions [12, 13]. The emergence of the high pressure gasoline fuel injection pump and advanced control strategies makes it possible for the DISI engines to adopt the multi-hole nozzles again. Downsizing the nozzle hole diameter, increasing nozzle hole number and injection pressure will lead to a better fuel atomization and spatial distribution [12], which will result in a better engine performance and a lower emission level. However, if the number of nozzle holes is too large, the interaction between the adjacent jets will occur. In addition, in the spray-guided DISI engine with a side-mounted injector, to avoid the wall impingement and to form a favorable mixture, non-axisymmetric nozzle hole arrangement, which means the included angles between two adjacent jets are different in one nozzle, is favorable. The results of the interactions of two adjacent jets are very important for this kind of application. In some circumstances the long spray tip penetration is suitable for a better air utilization, while in some other circumstance the short penetration is suitable for avoiding the wall impingement. The vaporization process of the spray is also very important because it will affect not only the ignition stability, but also the flame propagation. Many investigations on the impinging jets concerning the fundamental droplet–droplet and jet–jet interactions have been published [14–17], providing us useful information about the collision and coalescence behaviors of the droplets. Recently, the spray and mixture formation processes of group-hole nozzles in diesel engines have been studied both experimentally and numerically [18–23]. Compared with the conventional multi-hole nozzle, in which a single nozzle hole has the same flow area as the group of holes, the group-hole nozzle tends to provide the similar spray tip penetration, smaller SMD, higher air entrainment and larger vaporization ratio. However, due to the difference in the ignition method, the requirements of the DISI engines on the mixture formation process differ from that of the diesel engines. Furthermore, these papers mainly focused on the behaviors and phenomena. The mechanism of the behavior of the very near spray jets is still unclear.

The effect of spray impingement on the combustion process and emission in direct injection diesel engine was studied previously and the results show that high turbulence intensity and average wall temperature in cylinder induced enhanced air/fuel mixing and intensified evaporation of wall film decreases soot in impinging zones [24].

Summarizing the situation today, it must be pointed out that the predictive quality of the models currently used in CFD codes has already reached a very high level, and that the use of CFD simulations for the research and development activities of engine manufacturers with respect to the design of new and enhanced mixture formation and combustion concepts is not only practical but already necessary.

In this work, the effect of interaction between the adjacent jets on the vaporization process, vapor and liquid mass distributions, spray tip penetration, droplet spatial distribution and the deformation of the spray jets is clarified with more details in the DISI engine with the two-hole nozzle side-mounted injector by using the computational fluid dynamics (CFD) simulation.

2. Flow Field Equations

The Equations used by numerical model are as follows:
Continuum equation:

$$\frac{\partial \rho}{\partial t} = -\frac{\partial}{\partial x_j}(\rho U_j) \tag{1}$$

Momentum equation:

$$\rho\frac{\partial U_i}{\partial t} + \rho U_i \frac{\partial U_i}{\partial x_j} = \rho g_i - \frac{\partial P}{\partial x_i} + \frac{\partial}{\partial x_j}\left[\mu\left(\frac{\partial U_i}{\partial x_j} + \frac{\partial U_j}{\partial x_i} - \frac{2}{3}\frac{\partial U_k}{\partial x_k}\delta_{ij}\right)\right] \tag{2}$$

Energy Equation:

$$\rho\left(\frac{\partial H}{\partial t} + U_j \frac{\partial H}{\partial x_j}\right) = \rho \dot{q}_g + \frac{\partial P}{\partial t} + \frac{\partial}{\partial x_i}\left(U_j \tau_{ij}\right) + \frac{\partial}{\partial x_j}\left(\lambda \frac{\partial T}{\partial x_j}\right) \tag{3}$$

$\kappa - \varepsilon$ Turbulent equation:

$$\rho\frac{\partial k}{\partial t} + \rho U_j \frac{\partial k}{\partial x_j} = P + G - \varepsilon + \frac{\partial}{\partial x_j}\left(\mu + \frac{\mu_t}{\sigma_k}\frac{\partial k}{\partial x_j}\right) \tag{4}$$

$$\rho\frac{D\varepsilon}{Dt} = \left(C_{\varepsilon 1}P + C_{\varepsilon 3}G + C_{\varepsilon 4}k\frac{\partial U_k}{\partial x_k} - C_{\varepsilon 2}\varepsilon\right)\frac{\varepsilon}{k} + \frac{\partial}{\partial x_j}\left(\frac{\mu_t}{\sigma_\varepsilon}\frac{\partial \varepsilon}{\partial x_j}\right) \tag{5}$$

$$P = -2\mu_t S : S - \frac{2}{3}\left[\mu_t (trS) + K\right](trS) \tag{6}$$

$$G = -\frac{\mu_t}{\rho\sigma_\rho}\nabla\rho \tag{7}$$

$$\mu_t = C_\mu \rho \frac{k^2}{\varepsilon} \tag{8}$$

That the constant coefficients above quationse have shown in table 1.

Table 1. Constant coefficients

C_μ	$C_{\varepsilon 1}$	$C_{\varepsilon 2}$	$C_{\varepsilon 3}$	$C_{\varepsilon 4}$	σ_k	σ_ε	σ_ρ
0.09	1.44	1.92	0.8	0.33	1	1.3	0.9

3. Spray Model

Wave breakup model is used which is further modified to account for spray wall impingement effects, and is also improved by considering droplet distortion to obtain dynamically varying drop drag coefficients [25]. The initial fuel droplets have the diameter of nozzle hole which is technically called blob injection.

Droplet dissipation rate is modeled by the following equation:

$$\tau = \frac{3.726.C_2.r}{\Lambda\Omega} \tag{9}$$

In which Λ and Ω are wave length and wave growth rate and are functions of droplet characteristics and critical Weber number. Also droplet radius is assumed to obey the equation at steady state. Detailed information can be found in reference [26-27].

$$r_{stable} = \min\left\{\left(3\pi^2.U/2\Omega\right)^{0.33}, \left(3r^2\Lambda/4\right)^{0.33}\right\} \tag{10}$$

4. Computational Model

Numerical simulation was performed using the CFD code AVL FIRE 8.3. A cylindrical calculation domain with a diameter of 50 mm and a height of 80 mm was set up and was meshed with Fame Hybrid. The nozzle tips were set at the top center of the cylinder. The cells in the central part of the cylinder were refined so that the initial part of the spray can be described precisely. The size of cells varies from 0.5 to 2 mm. The standard k–ε turbulence model was used in the simulations of this study. Despite numerous shortcomings, which have been discovered over the past three decades of use and validation, it is generally accepted that the k– ε model usually yields reasonably realistic predictions of major mean-flow features in most situations. The Dukowicz evaporation model was solved by applying semi-empirical functions to the heat transfer combined with a heat mass transfer analogy [28]. For the sprays injected from hole-type nozzles, there are two methods to simulate the breakup processes. The first one is to set the initial particle size same as the nozzle hole diameter and to activate breakup models. The particle size is calculated using the primary and secondary breakup models. The second method is to set the initial particle size much smaller than the nozzle hole diameter and to assume that the disintegration process of the spray is completed right after the fuel injected out of the nozzle hole exits. The only recommended breakup model in this CFD code for GDI multi-hole injections is Huh–Gosman model.

This is clear evidence that liquid breakup and air entrainment occur very close to the nozzle exit, which means instantaneous atomization happens there. Since there was no suitable instantaneous atomization breakup model for gasoline sprays injected from multi-hole nozzles, the second method was adopted in this calculation. Schmidt particle interaction model was employed to simulate the collision and coalescence processes in the sprays. In comparison to O'Rourke and Bracco model [29], a presorting algorithm of the particles is adopted in Schmidt model to improve the calculation times considerably for high particle loads. For boundary conditions, all faces of the cylindrical calculation domain were set as ''walls", and all velocities in all directions were set to 0 m/s. A constant temperature of 500 K was set for all the ''walls". For initial conditions, all the cells in the domain were set to have a uniform initialization with the pressure of 1 MPa and temperature of 500 K. The initial density of the ambient gas was calculated according to the ideal gas law. The initial turbulence kinetic energy was 0.001 m2/s2 and the initial turbulence length scale was 0.001 m. The computational parameters are listed in Table 2.

Table 2. Computational conditions

Ambient gas	Air
Ambient temperature [K]	500
Ambient pressure [MPa]	1.0
Fuel	n-Octane
Fuel temperature [K]	300
Hole diameter [mm]	0.15
Number of holes	1, 2
γ for two-hole nozzle [deg]	5, 10, 15, 20, 25, 30
θ_0 spray angle [deg]	5, 10, 15, 20, 25, 30
Injection quantity [mg]	1.88
Injection duration [ms]	1.3
Time step [ms]	0.1
Calculation period [ms]	2.3 (1 ms AEOI)
Turbulence model	k–ε
Evaporation model	Dukowicz
Particle interaction model	Schmidt

Fig. 1 shows the definition of spray angle (θ_0) and the hole-axis-angle (γ) of the two-hole nozzle and single-hole nozzle spray.

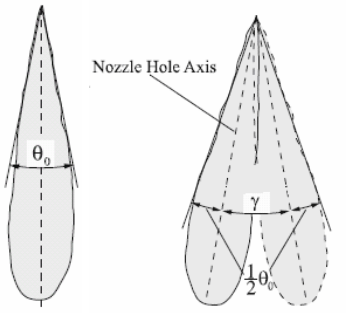

Fig.1 Definition of spray angle (θ_0) and hole-axis angle (γ)

5. Validation and grid indepency

A single-hole 0.25mm diameter orifice nozzle, used by Mirza [30], is chosen as a reference case and use is made of his published experimental results on fuel injection characteristics of the pump-line-injector combination using distribution type commercial fuel pump.

The grid used in the present analysis is 100000 cells .Grids having 150000 and 200000 configurations are also tested. As all grid configurations yield similar values of spray penetration, the 100000 grid is accepted as sufficiently fine. This grid size is also validated using experimental data in the next section.

The simulation results on spray penetration are compared with numerical solution. Figure 2 shows comparison of the predictions of numerical solution and the experimental results of Mirza [30]. The simulation results show very good agreement with the experimental results about the spray tip penetration tendency.

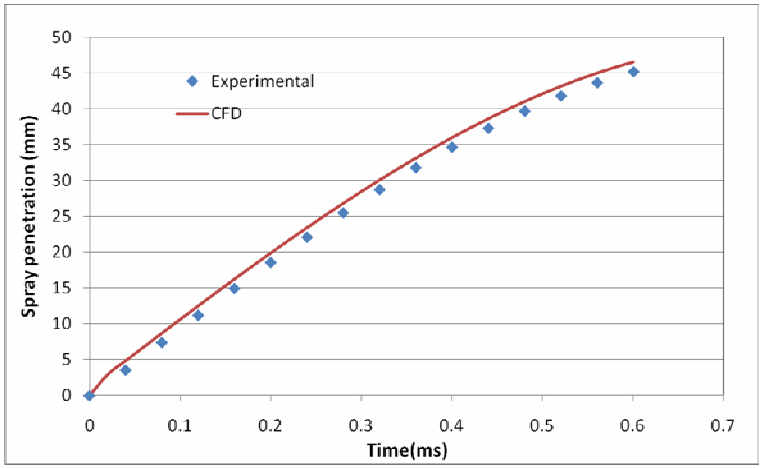

Fig. 2: Comparison of prediction and experiment [30]

6. Results and discussion

Fig. 3 and 4 shows the computational results of droplet distributions and tip penetration with spray cone angle (θ_0) and times in the single-hole injection system. Results show an increase in tip penetration as a result of an increase in time and decrease in θ0. Increased spray cone angle results faster fuel-air mixing, increased air entrainment and reduced spray penetration.

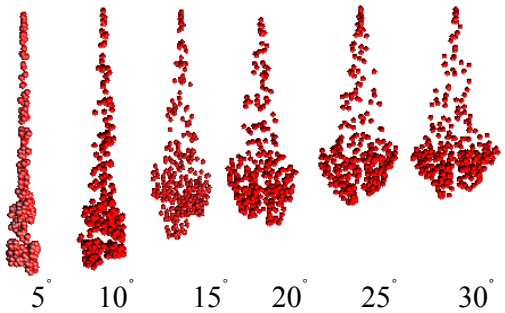

Fig. 3. Calculated droplets distribution of single-hole nozzle for θ_0= 5 to 30 deg

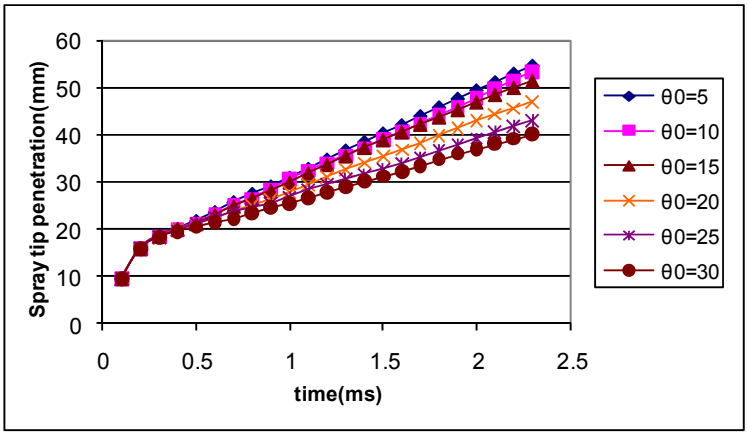

Fig. 4. The calculated spray tip penetrations at single-hole with the θ_0 of 5° to 30°

Also Fig. 3 shows the tip penetration distributions versus time of the single-hole injection with the θ_0 of 5˚ to 30˚. As can be seen from this curve, the tip penetration increases with an increase in time of start injection and decreases in cone angle.

Fig. 5 shows the spray tip penetration by using the numerical simulation results for the single-hole nozzle spray with the cone angle from θ_0= 5 to 30 deg in the end of injection. As shown this figure when spray cone angle increases, spray tip penetration decreases.

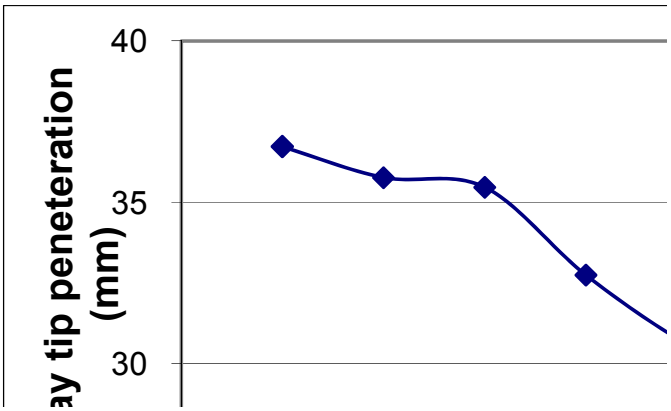

Fig.5. Change of spray tip penetration with respect to spray angle (t = 0 ms AEOI and mf = 1.88 mg for single-hole nozzle)

Fig. 6 and 7 illustrates the numerical results of SMD for sprays injected from single-hole nozzle at different spray angles (θ_0) versus time. As shown with the increase time and decrease spray angles, the Sauter mean diameter decreased. The comparison of fig.6 and 7 with fig.5, it is clear that with the decreasing of spray cone angle and increasing time spray tip penetration increases because large droplet formation.

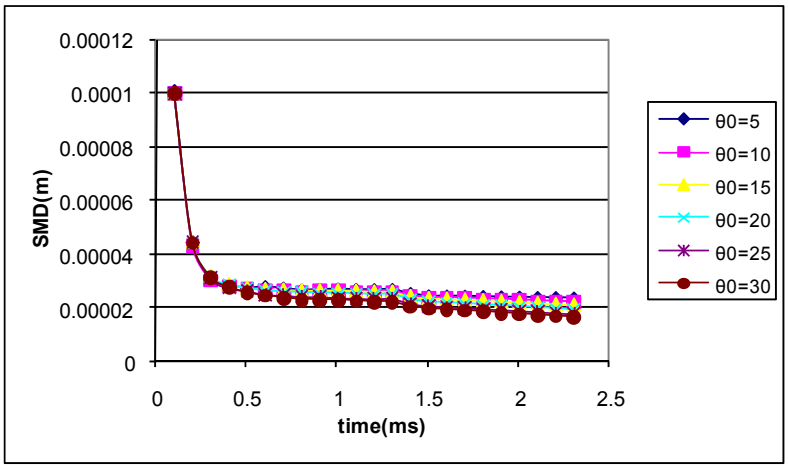

Fig. 6. The variation Sauter mean diameter versus time for different spray angles

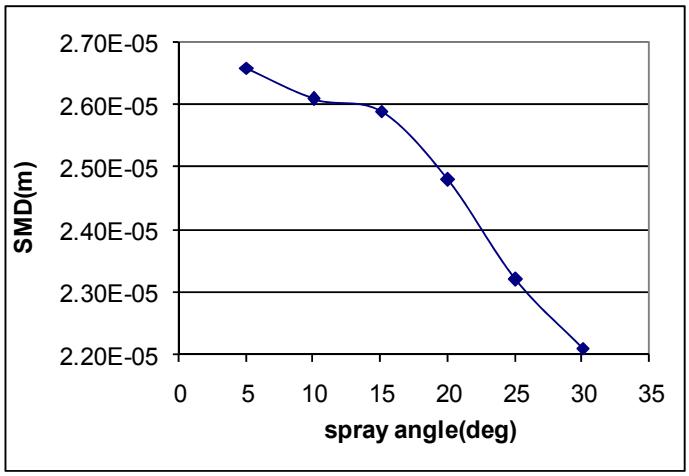

Fig.7. The effects of spray angle on the Sauter mean diameter for single hole nozzle (t = 0 ms AEOI)

Fig. 8 shows the numerical results of the sprays with spray angle of two-hole nozzles of 5 deg to 30 deg for γ =15 deg.

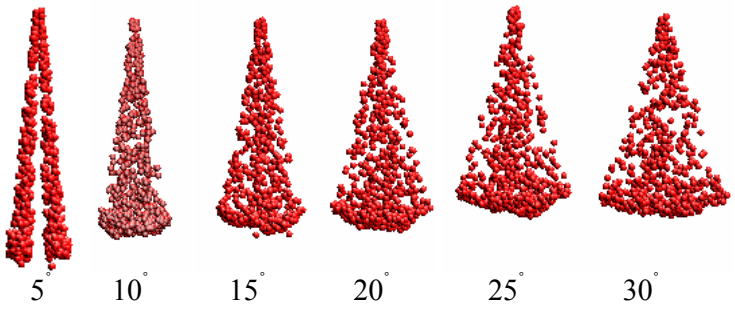

Fig. 8. Calculated droplets distribution of two-hole nozzle sprays for γ=15 deg and θ_0= 5 to 30 deg

Fig. 9 shows the variation of tip penetration with time for different spray angles in γ=15 deg. Results shows that spray tip penetration increases with decreasing θ_0 and increasing time.

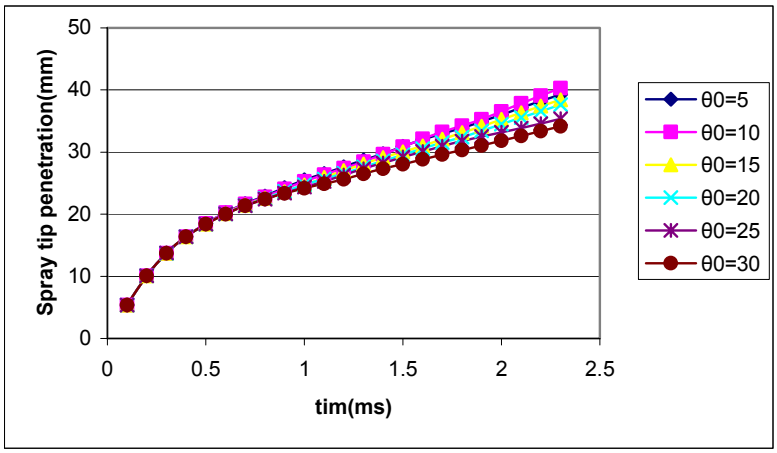

Fig. 9. Variation of spray tip penetration with time for different θ_0 (γ=15°)

Fig 10 illustrates the numerical results of SMD for sprays injected from two-hole nozzles at different spray angles (θ_0) versus time. As shown with the increase time and spray angles, the Sauter mean diameter decreased.

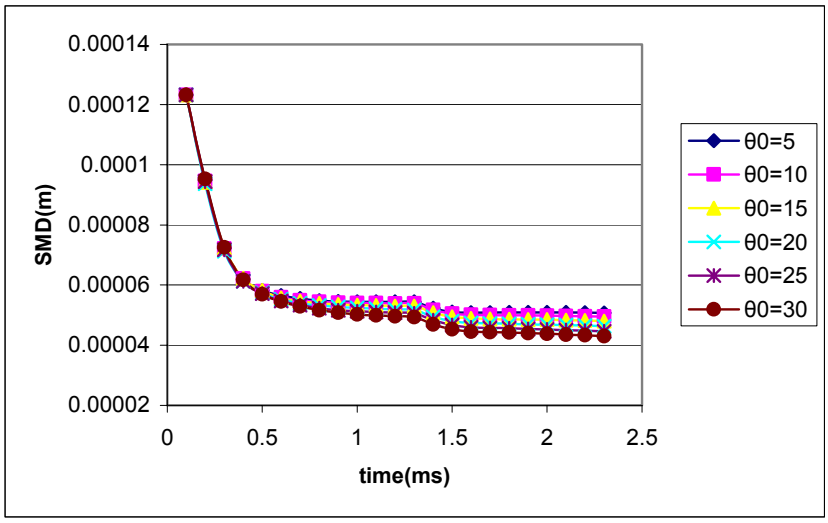

Fig. 10. The variation Sauter mean diameter versus time for different spray angles and hole-axis-angle (γ=15°)

Fig. 11 shows the numerical results of the sprays with spray angle of two-hole nozzles (θ_0) of 5 deg to 30 deg for γ=30 deg.

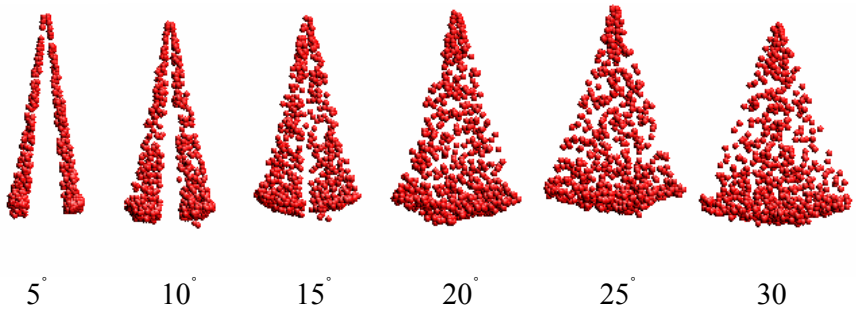

Fig.11. Calculated droplets distribution of two-hole nozzle sprays for γ=30 deg and θ0= 5 to 30 deg

Fig. 12 shows spray tip penetration with time for hole-axis angle (γ) is variable. Spray tip penetration increases considerably with increasing time and decreasing hole-axis angle.

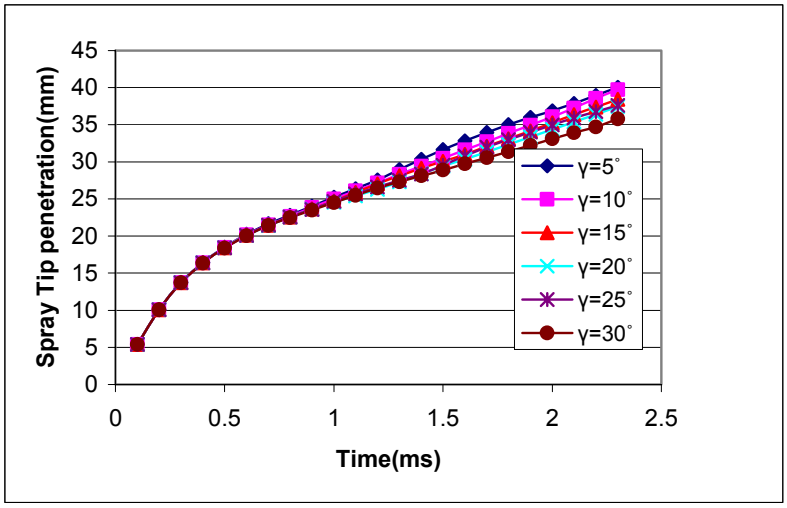

Fig.12. The variation spray tip penetration versus time for the case of spray angle of 15 deg for γ=5 to 30 deg

Fig. 13 illustrates the numerical results of spray tip penetrations for sprays injected from single and two-hole nozzles at different spray angles(θ_0) and hole-axis-angle(γ) for timing(t = 0 ms AEOI). The spray with the θ_0 of 5 deg for single hole nozzle had the longest spray tip penetration and the spray with the γ = 30 and θ_0 =30 deg had the shortest spray tip penetration under the same conditions.

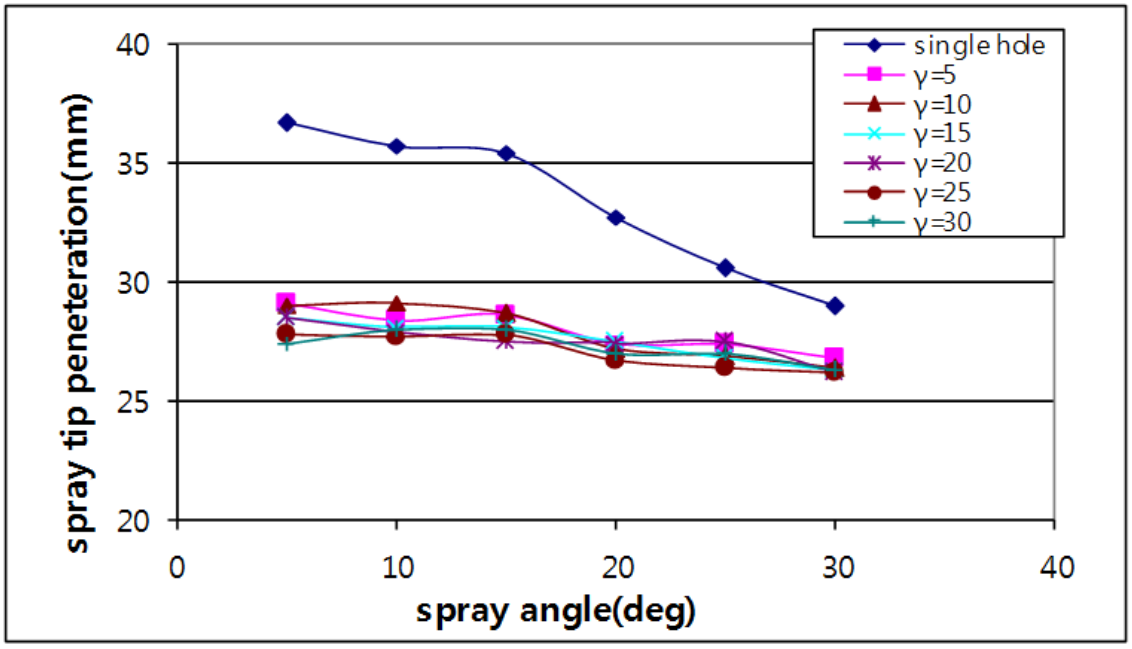

Fig.13. Spray tip penetration ratio of vapor mass to total fuel mass (t = 0 ms AEOI, Mf = 1.88 mg) for single-hole nozzle and two-hole nozzles

Fig. 14 show the values of SMD for $\gamma = 30^{\circ}$ cases with $\theta_0 = 5$, 10, 15, 20, 25 and 30. It can be seen that the increase of θ_0 and time makes SMD decrease.

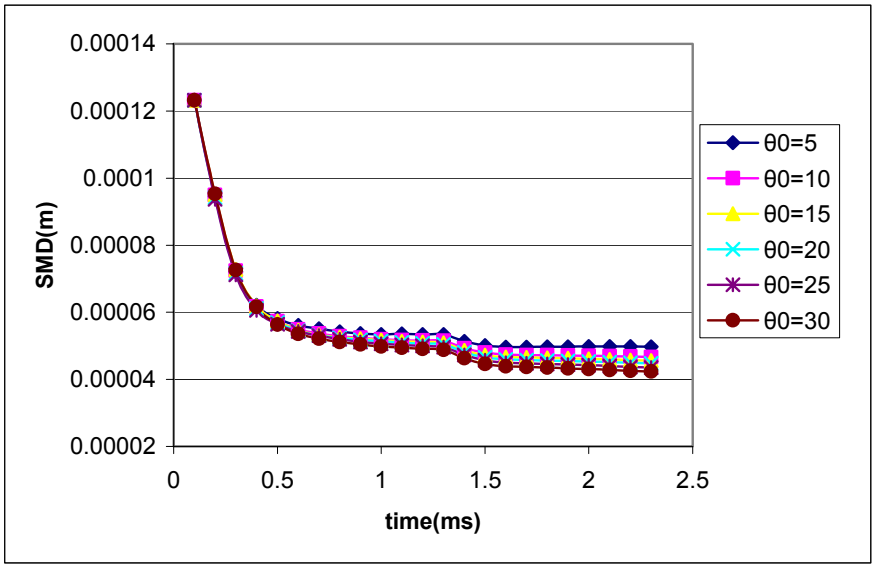

Fig. 14 the variation Sauter mean diameter versus time for different spray angles and hole-axis-angle (γ=30˚)

Fig. 15 shows, Sauter mean diameter (SMD) calculated as function of spray angle (θ0) for various hole-axis-angles. In general increasing the spray angle and hole-axis angle cause decreases the Sauter mean diameter.

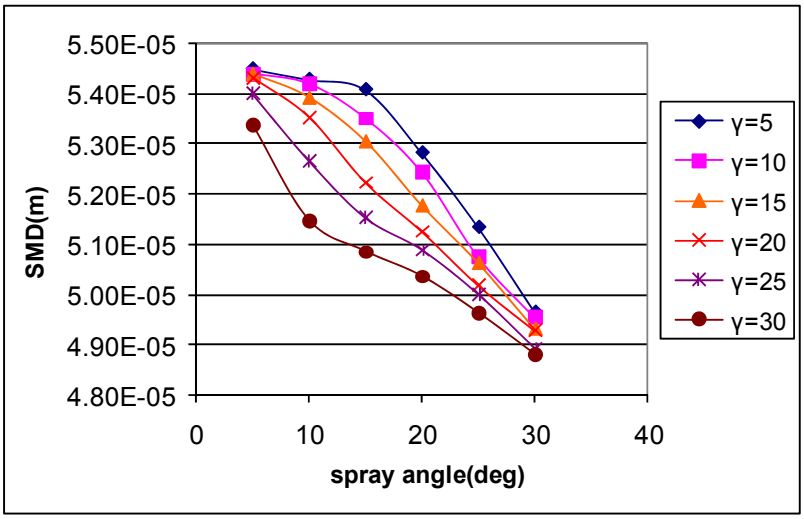

Fig. 15. Influence spray angle and hole axis angle on SMD (t= 0 ms AEOI)

Fig. 16 shows the measured ratios of vapor mass to total fuel mass (mv / mf) for single hole nozzle sprays at different spray angle and at two timings (0 and 0.5 ms AEOI). All the results show that, with the increase in spray angle (θ_0), the ratio of vapor mass to total fuel mass increased. At the two timings, the ratio of vapor mass to total fuel mass was increased with increasing the spray angle. The ratio of vapor mass to total fuel mass at 0.5 ms(AEOI) two times than the start of injection times.

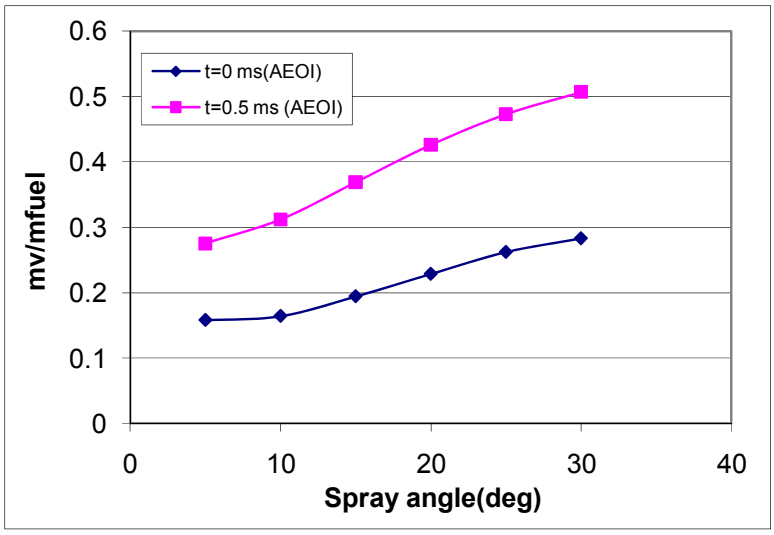

Fig.16. The ratio of vapor mass to total fuel mass (t = 0 and 0.5 ms AEOI) for single-hole nozzle

Fig. 17 shows the computational results of ratio of vapor mass to total fuel mass for 0 and 0.5 ms AEOI. Results show that the two-hole nozzles sprays had the smallest ratio of vapor mass to total fuel mass. This indicated that the single-hole nozzle spray increased the ratio of vapor mass to total fuel mass. As shown this figure because of lower SMD droplet formation and fast evaporation, the ratio of vapor mass to total fuel mass increases with increasing of cone angle and time

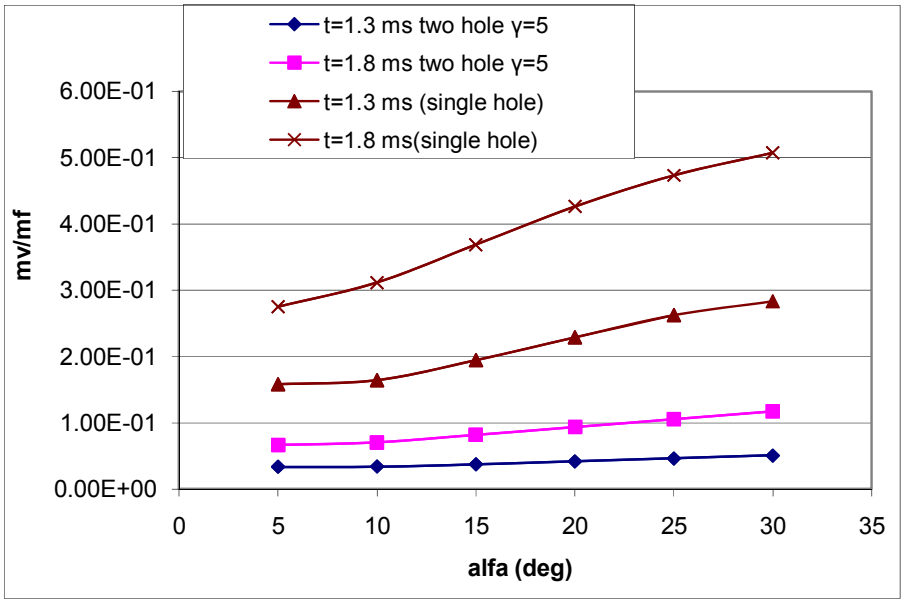

Fig.17. The ratio of vapor mass to total fuel mass versus spray angle (Mf = 1.88 mg)

Fig. 18 displays the influence of spray angle (θ_0) and hole-axis-angle (γ) on mv/mf. Results show that, increasing either of γ or θ_0 increases ratio of total vapor phase mass to total fuel mass.

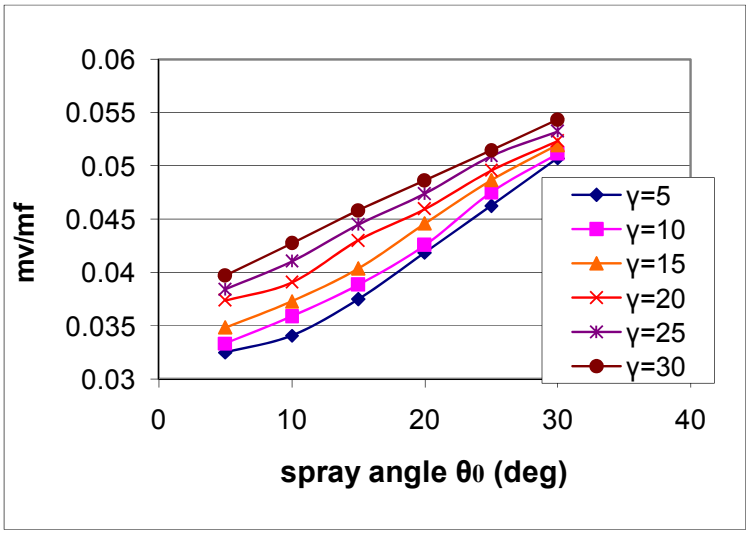

Fig. 18. The influence of spray angle on the mv/mf over different hole-axis-angle (t = 0 ms AEOI and Mf = 1.88 mg for two-hole nozzle)

7. Conclusions

Numerical simulation was performed using the CFD code AVL FIRE 8.3. in this work the effects of hole axis angle and spray cone angle on Spray characteristics for single-hole and two-hole nozzle were examined of spray tip penetration, and Sauter mean diameter using CFD simulation code. Other characteristics, including the vapor phase concentration distribution, droplet spatial distribution were acquired from the numerical simulation results. Based on the computational results, the following conclusions can be obtained:

1- The single-hole nozzle spray with the θ_0 of 5 deg had the longest spray tip penetration. The coalescences of droplets made the spray tend to get the longer spray tip penetration.

2- In the comparison with the two-hole nozzle spray, the single-hole nozzle spray with the θ0 of 5 deg had the longest spray tip penetration and for the two-hole nozzle spray with the γ of 30 deg and θ0 of 30 deg had the shortest spray tip penetration. When the hole–axis-angle (γ) increased from 5 to 30 deg, spray tip penetration remained almost constant.

3- For a single-hole nozzle spray, with the increase in spray angle (θ_0), the ratio of vapor mass to total fuel mass increased.

4- For a two-hole nozzle spray, the coalescences of the droplets made the ratio of vapor mass to total fuel mass smaller than that of the single-hole nozzle spray. A smaller hole–axis-angle (γ) resulted in a smaller ratio of vapor mass to total fuel mass under all conditions. Also with increasing spray angle (θ_0) and hole–axis-angle (γ) the ratio of vapor mass to total fuel mass increased.

5- When the spray angle (θ_0) and hole–axis-angle (γ) increased from 5 to 30 deg, the Sauter mean diameter (SMD), decreased for single-hole and two-hole nozzles used in this study.

Nomenclature

AEOI	After the end of injection
m_f	Total fuel mass, mg
m_v	Total vapor phase mass, mg
P_a	Ambient pressure, MPa
T_a	Ambient temperature, K
γ	Hole axis angle, deg
θ_0	Spray angle of single-hole nozzle, deg
SMD	Sauter mean diameter, m
t	time(ms)
U	Velocity
k	Kinetic Energy
ε	Dissipation

Reference

[1] F.F. Zhao, D.L. Harrington, M.C. Lai, Automotive Gasoline Direct-Injection Engines, SAE, 2002.

[2] F.Q. Zhao,M.C. Lai, D.L. Harrington, A review of mixture preparation and combustion strategies for spark-ignited direct injection gasoline engine, SAE 970627.

[3] Y. Tagagi, The role of mixture formation in improving fuel economy and reducing emissions of automotive S.I. engines, FISITA Technical Paper No. P0109, 1996.

[4] Preussner C, Kampmann S. Gasoline direct injection, a new challenge for future gasoline control systems – part 2: injector and mixture formation. MTZ 1997;58.

[5] Iwamoto Y, Noma K, Yamaguchi T, Ando H. Development of gasoline direct injection engine. SAE Paper 970541; 1997.

[6] Koike M, Saito A, Terutoshi Tomoda, Yamamoto Y. Research and development of a new direct injection gasoline engine. SAE Paper 2000-01-0530; 2000.

[7] Han Z, Yi J, Trigui N. Stratified mixture formation and piston surface wetting in a DISI engine. SAE Paper 2002-01-2655; 2002.

[8] Stevens E, Steeper R. Piston wetting in an optical DISI engine: fuel films, pool fires, and soot generation. SAE Paper 2001-01-1203; 2001.

[9] Eichlseder H, Baumann E, Muller P, Neugebauer S. Potential and risks of gasoline direct injection engines for passenger cardrivelines. MTZ worldwide 2000;61:2–5.

[10] Katashiba H, Honda T, Kawamoto M, Sumida M, Fukutomi N, Kawajiri K. Improvement of center injection spray guided DISI performance. SAE Paper 2006-01-1001; 2006.

[11] Ortmann R, Arndt S, Raimann J, Grzeszik R, Würfel G. Methods and analysis of fuel injection, mixture preparation and charge stratification in different direct injected SI engines. SAE Paper 2001-01-0970; 2001.

[12] Alperstein M, Schafer GH, Villforth III FJ. Texaco's stratified charge engine -multifuel, efficient, clean, and practical. SAE Paper 740563; 1974.

[13] Fujieda M, Siraisi T, Oosuga M. Influence of the spray pattern on combustion characteristics of the direct injection SI engine. Proc. ILASS-Japan (in Japanese), 1995.

[14] Abraham J, Khan A, Magi V. Jet–jet and jet–wall interactions of transient jets from multi-hole injectors. SAE Paper 1999-01-0513; 1999.

[15] Arai M, Saito M. Atomization characteristics of jet-to-jet and spray-to-spray impingement systems. Atom Sprays 1999;9:399–417.
[16] Ashgriz N, Poo JY. Coalescence and separation in binary collisions of liquid drops. J Fluid Mech 1990;221:183–204.
[17] Qian J, Law K. Regimes of coalescence and separation in droplet collision. J Fluid Mech 1997;331:59–80.
[18] Nishida K, Nomura S, Matsumoto Y. Spray and mixture properties of grouphole nozzle for D.I. diesel engines. in: Proceeding of ICLASS, 2006.
[19] Gao J, Matsumoto Y, Namba M, Nishida K. Group-hole nozzle effects on mixture formation and in-cylinder combustion processes in direct-injection diesel engines. SAE Paper 2007-01-4050; 2007.
[20] Gao J, Matsumoto Y, Nishida K. Effects of group-hole nozzle specifications on fuel atomization and evaporation of direct injection diesel sprays. SAE Paper 2007-01-1889; 2007.
[21] Zhang YY, Nishida K, Nomura S. Spray characteristics of a group-hole nozzle for direct-injection diesel engines. Atom Sprays 2006;16:35–49.
[22] Park SW, Reitz RD. Modeling the effect of injector nozzle-hole layout on diesel engine fuel consumption and emissions. J Eng Gas Turb Power-Trans ASME 2008;130:032805-1–10.
[23] Matsumoto A, Xie X, Lai MC, Deere J. Characterization of diesel common rail spray behavior for single- and double-hole nozzles. SAE Paper 2008-01-2424; 2008.
[24] Jafarmadar. S, Khalil arya. Sh, Shafee. S, Barzegar. R, "Modeling the effect of spray/wall impingement on combustion process and emission of DI diesel engine", Journal of Thermal Science: Vol. 13 (2009), No. 3, pp. 23-34.
[25] A. Uludogan, D. E. Foster, and R. D. Reitz "Modeling the Effect of Engine Speed on the Combustion Process and Emissions in a DI Diesel Engine" SAE paper 962056.
[26] Tomoyuko Wakisaka,Kunikazo Ibaraki "An improvement droplet breakup model for three dimensional diesel spray simulation ." rd 3 KSME, JSME, Thermal Engineering Conference 11-167-162, 1996.
[27] Carsten Baumgarten, "Mixture Formation in Internal Combustion Engines", Springer-Verlag Berlin Heidelberg 2006.
[28] Dukowicz JK. Quasi-steady droplet change in the presence of convection, informal report Los Alamos Scientific Laboratory. Rep. LA7997-MS.
[29] O'Rourke PJ, Bracco FV. In: IMechE –stratified charge automotive engines conference, 1980.
[30] Mirza, M. R., "Studies of Diesel sprays interacting with cross flows and solid boundaries", PhD Thesis, UMIST UK 1991.

Affiliations

- Samad JAFARMADAR*: Assistant Professor, Department of Mechanical Engineering, Urmia University, Urmia, Iran

- Vahied HEIDARPOOR: Phd student, Department of Mechanical Engineering, Urmia University, Urmia, Iran

* Corresponding author : s.jafarmadar@urmia.ac.ir